Article

Cell Reports

Immunometabolic Pathways in BCG-Induced Trained Immunity

Graphical Abstract

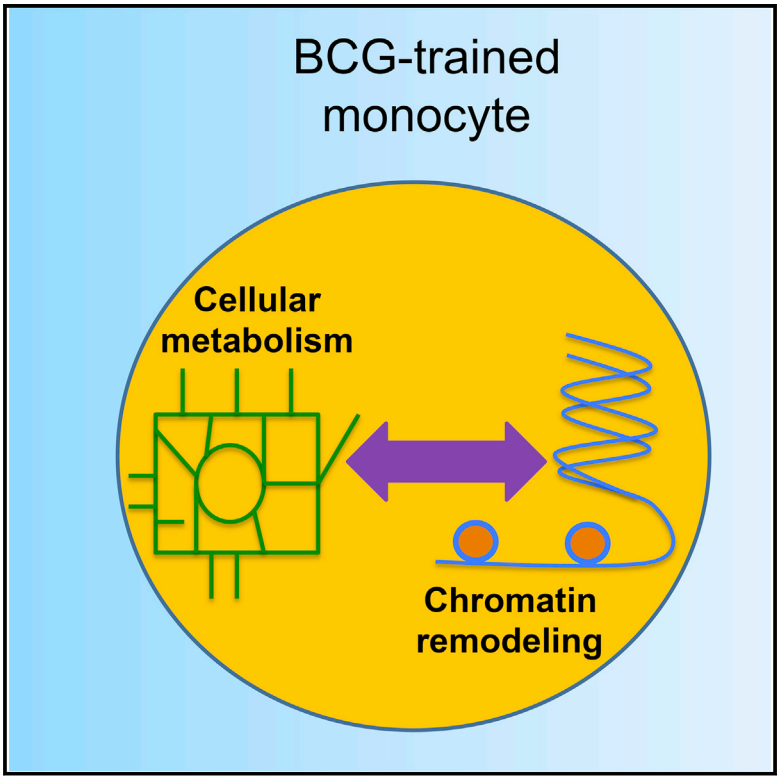

Authors

Rob J.W. Arts, Agostinho Carvalho, Claudia La Rocca, ..., Giuseppe Matarese, Reinout van Crevel, Mihai G. Netea

Correspondence

mihai.netea@radboudumc.nl

In Brief

Arts et al. found that glycolysis and glutamine metabolism, regulated by the Akt-mTOR pathway, are central mediators for the induction of trained immunity by BCG in monocytes. They show that metabolic changes are dependent on changes in histone modifications, which are influenced by metabolic changes.

Highlights

- Cellular metabolism undergoes major shifts in BCG-trained monocytes
- The Akt-mTOR signaling pathway is essential for these shifts in metabolism
- Induction of glucose and glutamine metabolism are crucial in trained immunity
- The metabolic changes are the result of rewiring of chromatin modifications

Arts et al., 2016, Cell Reports *17*, 2562–2571
December 6, 2016
http://dx.doi.org/10.1016/j.celrep.2016.11.011

CellPress

OPEN ACCESS
CellPress

Cell Reports
Article

Immunometabolic Pathways in BCG-Induced Trained Immunity

Rob J.W. Arts,[1] Agostinho Carvalho,[2,3] Claudia La Rocca,[4] Carla Palma,[5] Fernando Rodrigues,[2,3] Ricardo Silvestre,[2,3] Johanneke Kleinnijenhuis,[1] Ekta Lachmandas,[1] Luís G. Gonçalves,[6] Ana Belinha,[2,3] Cristina Cunha,[2,3] Marije Oosting,[1] Leo A.B. Joosten,[1] Giuseppe Matarese,[4,7] Reinout van Crevel,[1] and Mihai G. Netea[1,8,*]

[1]Department of Internal Medicine and Radboud Center for Infectious Diseases (RCI), Radboud University Medical Center, 6500 HB Nijmegen, the Netherlands
[2]Life and Health Sciences Research Institute (ICVS), School of Medicine, University of Minho, 4710-057 Braga, Portugal
[3]ICVS/3B's – PT Government Associate Laboratory, Braga/Guimarães, Portugal
[4]Istituto per l'Endocrinologia e l'Oncologia Sperimentale, Consiglio Nazionale delle Ricerche (IEOS-CNR), 80131 Napoli, Italy
[5]Department of Infectious, Parasitic and Immune-Mediated Diseases, Istituto Superiore di Sanità, 00161 Roma, Italy
[6]Instituto de Tecnologia Química e Biológica António Xavier, Universidade Nova de Lisboa, 2780-157 Oeiras, Portugal
[7]Dipartimento di Medicina Molecolare e Biotecnologie Mediche, Università di Napoli Federico II, 80131 Napoli, Italy
[8]Lead Contact
*Correspondence: mihai.netea@radboudumc.nl
http://dx.doi.org/10.1016/j.celrep.2016.11.011

SUMMARY

The protective effects of the tuberculosis vaccine *Bacillus Calmette-Guerin* (BCG) on unrelated infections are thought to be mediated by long-term metabolic changes and chromatin remodeling through histone modifications in innate immune cells such as monocytes, a process termed trained immunity. Here, we show that BCG induction of trained immunity in monocytes is accompanied by a strong increase in glycolysis and, to a lesser extent, glutamine metabolism, both in an in-vitro model and after vaccination of mice and humans. Pharmacological and genetic modulation of rate-limiting glycolysis enzymes inhibits trained immunity, changes that are reflected by the effects on the histone marks (H3K4me3 and H3K9me3) underlying BCG-induced trained immunity. These data demonstrate that a shift of the glucose metabolism toward glycolysis is crucial for the induction of the histone modifications and functional changes underlying BCG-induced trained immunity. The identification of these pathways may be a first step toward vaccines that combine immunological and metabolic stimulation.

INTRODUCTION

The live attenuated *Bacillus Calmette-Guerin* (BCG) vaccine confers protection against severe forms of *Mycobacterium tuberculosis* infection while having a limited effect against pulmonary tuberculosis (Colditz et al., 1994; Zumla et al., 2013). In addition to its effects on tuberculosis, it has also been shown that vaccination with BCG leads to non-specific protective effects against non-related infections and mortality. In observational studies in West Africa, it was shown that the presence of a BCG scar or PPD (purified protein derivative) positivity is associated with reduced child mortality (Garly et al., 2003; Roth et al., 2005). Furthermore, in two randomized controlled trials, early administration of the BCG vaccination reduced child mortality, mainly as a result of less neonatal sepsis and lower respiratory infections (Aaby et al., 2011; Biering-Sørensen et al., 2012; Kristensen et al., 2000). BCG is also used to treat bladder cancer and appears to be beneficial in treating several other diseases or conditions, such as warts, leishmaniasis, and asthma (Pereira et al., 2009; Rousseau et al., 2008; Salem et al., 2013). As further proof of its non-specific protective effects, BCG was shown to protect mice against lethal candidiasis (van 't Wout et al., 1992), and, interestingly, this protective effect was also present in SCID (severe combined immunodeficiency) mice, therefore showing that this non-specific protection is T and B cell independent (Kleinnijenhuis et al., 2012). It was found that these effects are mediated by the functional and epigenetic reprogramming of innate immune cells such as monocytes, macrophages, and NK (natural killer) cells, a process termed "trained immunity" (Netea et al., 2011, 2016).

We have recently demonstrated that induction of trained immunity by fungal components such as β-glucan leads to a shift of cellular metabolism from oxidative phosphorylation toward glucose fermentation (Cheng et al., 2014; Saeed et al., 2014). This is a process mediated through the Akt/mTOR (mammalian target of rapamycin)/HIF1α (hypoxia-inducible factor 1α) pathway, which is crucial for an effective induction of trained immunity (Cheng et al., 2014; Saeed et al., 2014). Similar observations on the importance of metabolic changes during immune cells activation have been made by others: proinflammatory—e.g., M(interferon [IFN]γ)—macrophages are characterized by increased glycolysis and lactate production, whereas the more anti-inflammatory—e.g., M(interleukin [IL]-4)—macrophages seem to rely on

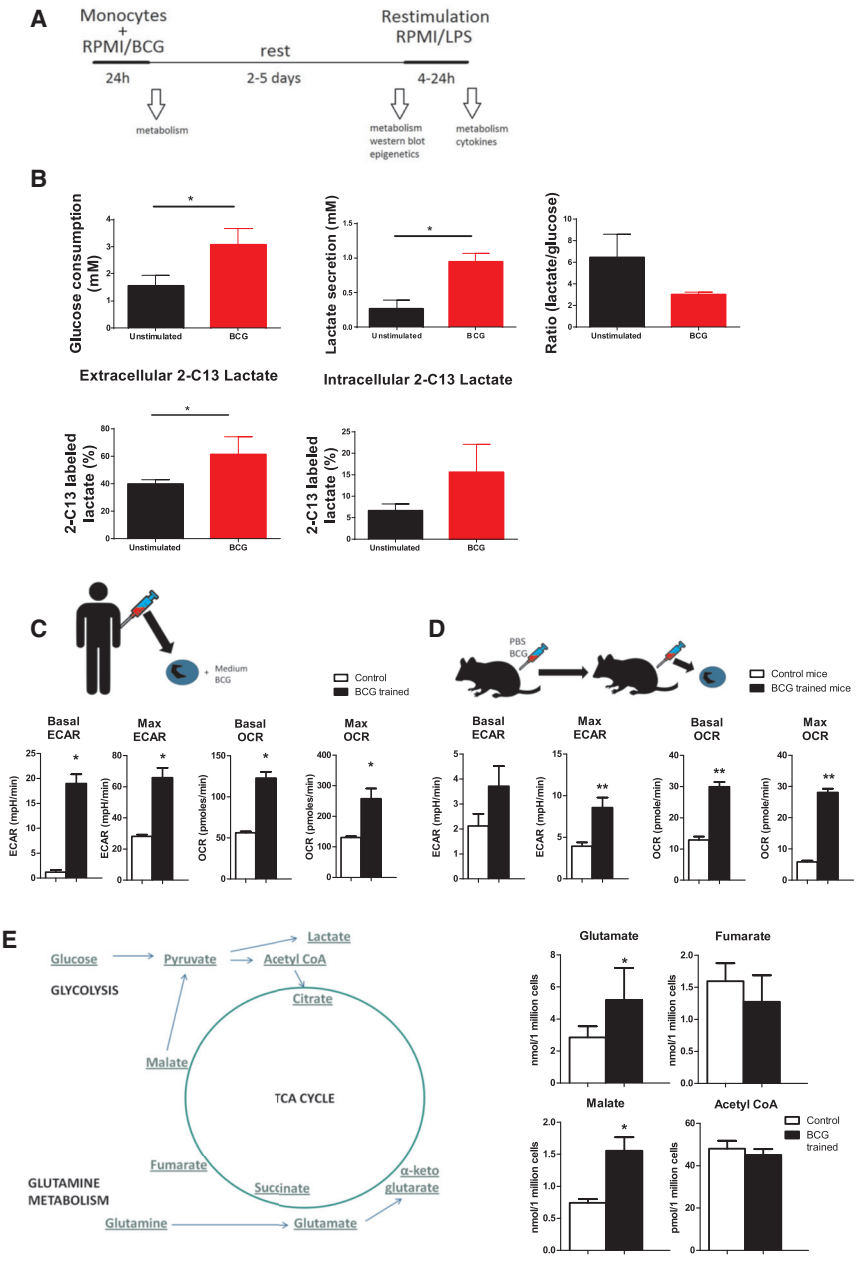

Figure 1. Role of Glucose Metabolism for the Induction of BCG-Induced Trained Immunity

(A) Graphical outline of the in vitro methods.

(B) Monocytes were incubated for 24 hr with culture medium or BCG and then allowed to rest for 2 days and stimulated for 24 hr with LPS in medium with ^{13}C-labeled glucose. Glucose consumption from the medium, lactate production, and their ratios were determined. Also, incorporation of the ^{13}C-label in lactate was determined (mean ± SD, n = 3). *p < 0.05, Student's t test.

(C) Monocytes were incubated for 24 hr with culture medium or BCG. At day 6 (prior to restimulation), extracellular acidification rate (ECAR) and oxygen consumption rate (OCR) were determined by Seahorse (mean ± SEM, n = 6). *p < 0.05, Wilcoxon signed-rank test.

(D) Mice were vaccinated with BCG. After 7 days, splenocytes were isolated, and ECAR and OCR were determined by Seahorse (mean ± SEM, n = 6). *p < 0.05; **p < 0.01, Mann-Whitney test.

(E) Monocytes were incubated for 24 hr with culture medium or BCG. At day 6 (prior to restimulation), intracellular concentrations of glutamate, fumarate, malate, and acetyl-CoA were determined (mean ± SEM, n = 6). *p < 0.05, Wilcoxon signed-rank test. See also Figures S1–S4.

oxidative phosphorylation, fatty acid uptake, and β-oxidation (Odegaard and Chawla, 2011). In contrast monocytes from patients suffering from sepsis-induced immunoparalysis show reduced pro-inflammatory cytokine production with a defective capacity to mount glycolysis and β-oxidation (Cheng et al., 2016).

So far, however, no data have been reported regarding cellular metabolism in BCG-induced trained immunity. In this study, we used in vitro and in vivo (both mice and human) models of trained immunity (Kleinnijenhuis et al., 2012) to assess the changes in cellular metabolism pathways that underlie BCG-induced trained immunity and its effects on cytokines and epigenetic (histone) changes. Deciphering the role of metabolic pathways for the non-specific effects of BCG vaccination may lead to a better understanding of the induction of trained immunity and how modulation of cellular metabolism pathways may be used to boost the effect of vaccines.

RESULTS

Glucose Is a Main Energy Source for BCG-Trained Monocytes

To assess glycolytic rate, a well-established in vitro method of trained immunity was used (Kleinnijenhuis et al., 2012; Quintin et al., 2012). Human monocytes were incubated for 24 hr with BCG, or RPMI medium as a control, and restimulated after a subsequent 5 days of rest with lipopolysaccharide (LPS) or RPMI medium for 24 hr (Figure 1A). Glycolytic rate was assessed by measuring glucose consumption from the medium, and lactate production was used to measure the fermentative capacity, 24 hr after LPS stimulation. Both glucose consumption and lactate release were increased, reflecting the induction of glycolysis (Figure 1B). The ratio of lactate:glucose in BCG-trained macrophages was close to 2, suggesting that these cells use glucose as the major source of lactate, whereas in non-trained macrophages (showing a higher ratio), other substrates were used as well (Figure 1B; Figure S1). As further proof, priming with BCG significantly increased incorporation of ^{13}C in lactate during the 24 hr of restimulation with LPS (Figure 1B; Figures S2A and S2B).

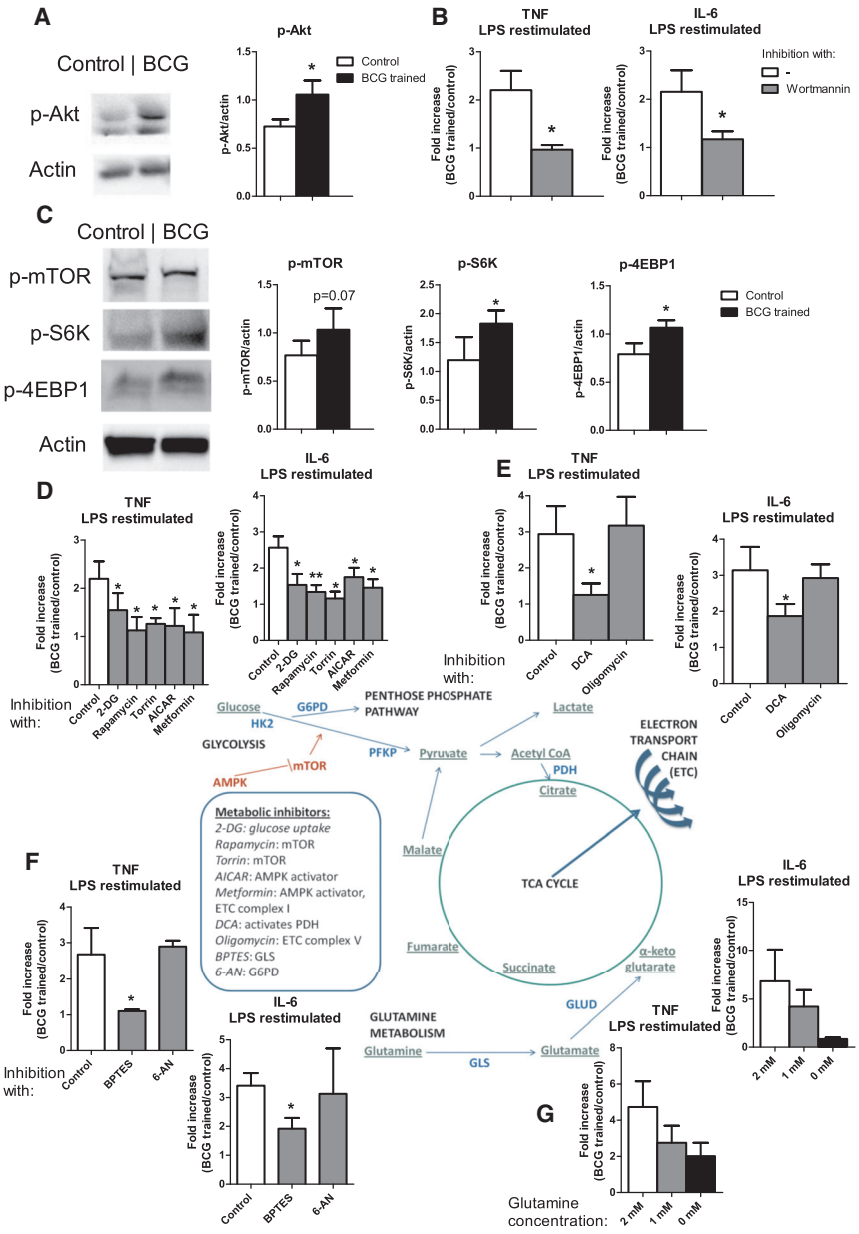

Figure 2. Akt/mTOR Activation and Induction of BCG-Induced Trained Immunity

(A) Monocytes were incubated for 2 hr with BCG or control medium, and phosphorylated Akt was assessed by western blot and quantified (mean ± SEM, n = 5). *p < 0.05, Wilcoxon signed-rank test.

(B) Monocytes were incubated for 24 hr with culture medium or BCG, with or without Wortmannin. At day 6, after restimulation with LPS, IL-6 and TNF-α concentrations in the supernatants were measured (mean ± SEM, n = 6). *p < 0.05, Wilcoxon signed-rank test.

(C) Monocytes were incubated for 24 hr with culture medium or BCG. At day 6 (prior to restimulation), phosphorylation of mTOR, S6K, and 4EBP1 was assessed by western blot and quantified (mean ± SEM, n = 5). *p < 0.05, Wilcoxon signed-rank test.

(D–F) Monocytes were incubated for 24 hr with culture medium or BCG, with or without the metabolic modulators of glycolysis/mTOR (D), TCA/OxPhos (oxidative phosphorylation) (E), glutamine metabolism or pentose phosphate pathway (PPP) (F). At day 6, IL-6 and TNF-α production was determined in the supernatants after restimulation with LPS (mean ± SEM, n = 6). *p < 0.05, Wilcoxon signed-rank test.

(G) Monocytes were incubated for 24 hr with culture medium or BCG. Culture media with 2, 1, or 0 mM of L-glutamine were used. At day 6, IL-6 and TNF-α production in the supernatants were determined after restimulation with LPS (mean ± SEM, n = 6). *p < 0.05, Wilcoxon signed-rank test.

Incorporation of ^{13}C-labels was also increased in rybosyl-1, which is suggestive of an induction of the pentose phosphate pathway (Figure S2C). Assessment of BCG-trained monocytes on day 6 (prior to restimulation) using Seahorse technology showed an increased basal and maximal extracellular acidification rate (ECAR) as a measure of lactate production. Interestingly, however, the oxygen consumption rate (OCR, as a measure for oxidative phosphorylation) was also increased (Figure 1C; Figure S3A). This is different compared to β-glucan trained macrophages, which have shown a classical Warburg effect (with increased glycolysis and decreased oxidative phosphorylation) (Cheng et al., 2014). These data were validated in mice, where BCG led to an upregulation of ECAR and OCR in splenocytes 1 week after vaccination (Figure 1D; Figure S3B).

Besides glucose, other metabolites can be used for energy and carbon metabolism. Therefore, we assessed amino acid utilization at several time points, but none were significantly increased (Figure S4). Interestingly, intracellular concentrations of glutamate and malate (but not fumarate), metabolites that can be produced from glutamine, were increased. In contrast, concentrations of acetyl-coenzyme A (CoA), a central metabolite linking glycolysis and fatty acid metabolism with trichloroacetic acid (TCA) cycle, were not modulated by BCG training (Figure 1E).

Metabolic Changes and Trained Immunity Are Dependent on Activation of the Akt-mTOR Pathway

We previously showed that the shift toward a higher glycolytic rate in β-glucan-induced trained monocytes is dependent on the Akt/mTOR pathway (Cheng et al., 2014). Supporting a similar pathway in BCG-induced trained immunity, we found that monocytes that were primed for 2 hr with BCG showed an increased Akt phosphorylation (Figure 2A). Inhibition of Akt by Wortmannin during the first 24 hr of BCG training abrogated the increase in cytokine production by LPS restimulation at day 6, confirming the essential role of Akt for induction of trained immunity

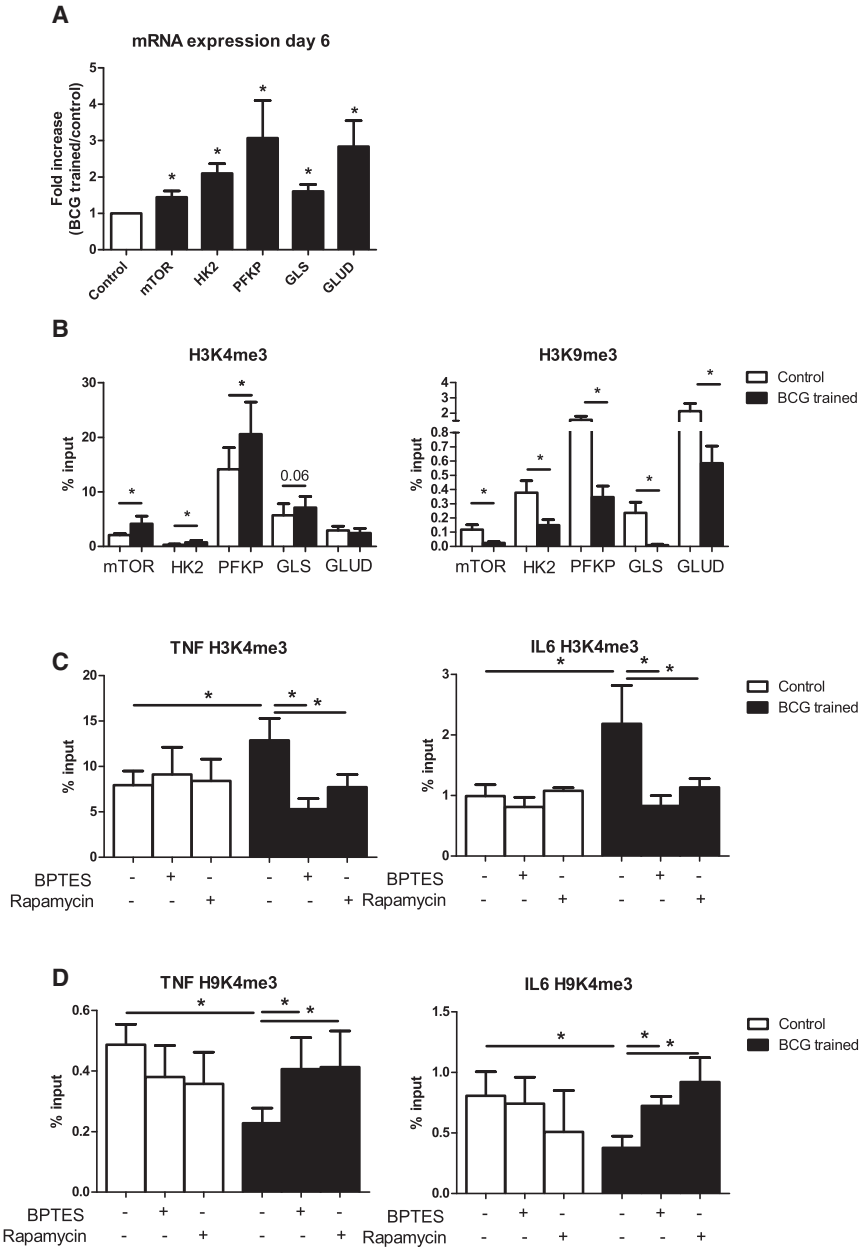

Figure 3. Epigenetic and Metabolic Regulation in BCG-Induced Trained Immunity

Monocytes were incubated for 24 hr with culture medium or BCG. At day 6 (prior to restimulation):

(A) mRNA expression of mTOR and two rate-limiting enzymes in glycolysis (HK2, and PFKP) and glutamine metabolism (GLS and GLUD) were determined (mean ± SEM, n = 6). *p < 0.05, Wilcoxon signed-rank test.

(B) DNA was isolated, and H3K4me3 and H3K9me3 were determined at promoter sites of *MTOR*, *HK2*, *PFKP*, *GLS*, and *GLUD* (mean ± SEM, n = 6). *p < 0.05, Wilcoxon signed-rank test.

(C and D) H3K4me3 (C) or H3K9me3 (D) was determined at promoter sites of *TNFA* and *IL6*. During the first 24 hr, inhibitors of glutamine metabolism (BPTES) or mTOR/glycolysis (rapamycin) were added (mean ± SEM, n = 6). *p < 0.05, Wilcoxon signed-rank test.

See also Table S1.

(Figure 2B). BCG-induced training of monocytes also led to the phosphorylation of mTOR and its targets S6K and 4EPB1, as determined at day 6 (Figure 2C), and inhibition of mTOR and glycolysis by rapamycin, torin, AICAR, and 2-deoxyglucose (2-DG) during BCG training abrogated the increased cytokine production (Figure 2D). Similar effects were observed with the addition of metformin that has more broad metabolic effects on both glycolysis and oxidative phosphorylation (Figure 2D). Addition to the medium of dichloroacetate (DCA), which inhibits pyruvate dehydrogenase kinases and, thus, shifts glucose metabolism toward the TCA cycle (Cairns et al., 2007), abrogated the induction of cytokine production. In contrast, the inhibition of the electron transport chain by the complex V inhibitor oligomycin did not have an effect on the induction of trained immunity (Figure 2E). Inhibition of glutamine metabolism by BPTES also abrogated cytokine production (Figure 2F). Decreasing glutamine concentration in the medium also inhibited the induction of cytokine production after restimulation with LPS (Figure 2G), showing that glutamine utilization is essential for the induction of trained immunity. Inhibition of the pentose phosphate pathway by 6-aminonicotinamide had no effect on the induction of training (Figure 2F). Thus, the Akt-mTOR pathway—which, in turn, drives glucose and glutamine metabolism—is crucial for BCG-induced trained immunity.

Epigenetic Regulation of Metabolism

To further assess how glucose and glutamine metabolism are regulated in BCG-trained monocytes and macrophages, mRNA expression of mTOR and four essential enzymes in glycolysis and glutamine metabolism were determined at day 6 after BCG training. mTOR and all four enzymes were upregulated in trained monocytes prior to restimulation (Figure 3A). To investigate whether this increased expression was a result of epigenetic changes, histone 3 trimethylation of lysine 4 (H3K4me3) and lysine 9 (H3K9me3) were determined. Both these two histone marks have been previously shown to be important in BCG-induced trained immunity, with H3K4me3 being a histone mark denoting open chromatin and increased gene transcription, while H3K9me3 is a repressor mark (Arts et al., 2015a, 2015b; Kleinnijenhuis et al., 2012). H3K4me3 was, indeed, found to be significantly increased at the promoters of mTOR, HK2, and PFKP, and the decrease of H3K9me3 was even more pronounced (also for

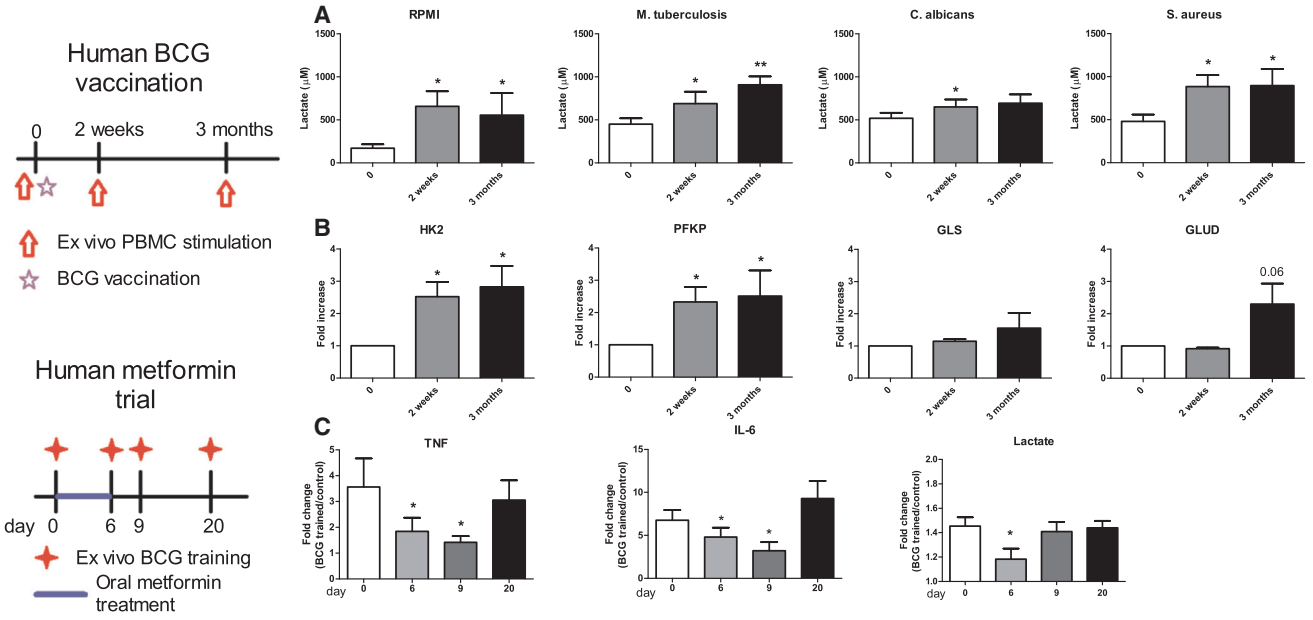

Figure 4. The Role of Glycolysis in Proof-of-Principle Clinical Trials in Human Volunteers

(A) In a human BCG vaccination trial (Kleinnijenhuis et al., 2012), healthy volunteers were vaccinated with BCG, and at baseline and after 2 weeks and 3 months, PBMCs were ex vivo restimulated, and lactate concentrations in the supernatants were assessed (mean ± SEM, n = 19). *p < 0.05, Friedman test and Dunn's post-test).

(B) In the same vaccination trial expression of HK2, PFKP, GLS, and GLUD were determined in PBMCs (mean ± SEM, n = 6). *p < 0.05, Wilcoxon signed-rank test.

(C) In a separate human metformin trial, healthy volunteers were treated for 6 days with an increasing dose of metformin. At baseline (day 0), directly after completed metformin treatment (day 6), and 3 days (day 9) and 14 day (days 20) after metformin treatment, monocytes were isolated and ex vivo trained with BCG (as shown in Figure 1A). TNF-α and IL-6 production after 24-hr restimulation with LPS were determined at day 7, and lactate production was assessed prior to restimulation (day 6) (mean ± SEM, n = 11). *p < 0.05, Wilcoxon signed-rank test.

GLS and GLUD) (Figure 3B). When monocytes were trained with BCG, an increase of H3K4me3 and a decrease of H3K9me3 were found at the promoters of *TNFA* and *IL6*, just as in previous findings (Arts et al., 2015a). However, when BCG training was inhibited with metabolic inhibitors of glutamine metabolism (BPTES) or mTOR/glycolysis (rapamycin), the epigenetic changes at the promoter site of *TNFA* and *IL6* were reversed to the baseline status (Figures 3C and 3D). This shows that the epigenetic and metabolic changes are intertwined and highly dependent on each other.

Induction of Glycolysis Is Crucial for Trained Immunity following BCG Vaccination of Human Volunteers

Next, we examined whether the increased cytokine production ex vivo 2 weeks and 3 months following BCG vaccination (Kleinnijenhuis et al., 2012) was accompanied by increased glycolysis. Indeed, this seemed to be the case, as shown by higher lactate concentrations in supernatants (Figure 4A) and higher expression of HK2 and PFKP in peripheral blood mononuclear cells (PBMCs), isolated from BCG-vaccinated individuals. Expression of GLS and GLUD, involved in glutamine metabolism, was not significantly affected by BCG vaccination, but there was a possible trend toward higher expression at 3 months (Figure 4B).

To examine these pathways in vivo, we next administered metformin, an AMPK (AMP-activated protein kinase) activator (and mTOR inhibitor), to healthy volunteers for 5 days and examined ex vivo induction of trained immunity with BCG (as shown in Figure 1A). The use of metformin inhibited the induction of trained immunity by BCG, as shown by a temporarily decreased induction of cytokine responses and lactate production upon secondary stimulation (Figure 4C).

Genetic Validation for a Role of Glycolysis Pathway in Trained Immunity

As a final step, we examined whether genetic variation in metabolic pathways affected in vitro training of monocytes by BCG: if glycolysis and glutaminolysis are important for the induction of trained immunity, then genetic variation of rate-limiting enzymes in these pathways should modulate trained immunity. In order to determine this, the effects of SNPs in mTOR, HK2, PFKP, GLS, and GLUD1/2 on induction of IL-6 and tumor necrosis factor α (TNF-α) after LPS restimulation of BCG-trained macrophages were determined in a first cohort (n = 65), and significant associations were confirmed in a second cohort (n = 49). SNPs in mTOR showed modulation of trained immunity, but as numbers of the homozygous genotypes were small and several mTOR SNPs were in linkage disequilibrium, it is hard to draw strong conclusions on the causative SNP (Figure S5). Three GLUD SNPs were not associated with the induction of cytokine production, and the effect observed in one of the two GLS SNPs (rs7564529) was not validated in the second cohort. However, three SNPs in HK2 and one SNP in PFKP significantly

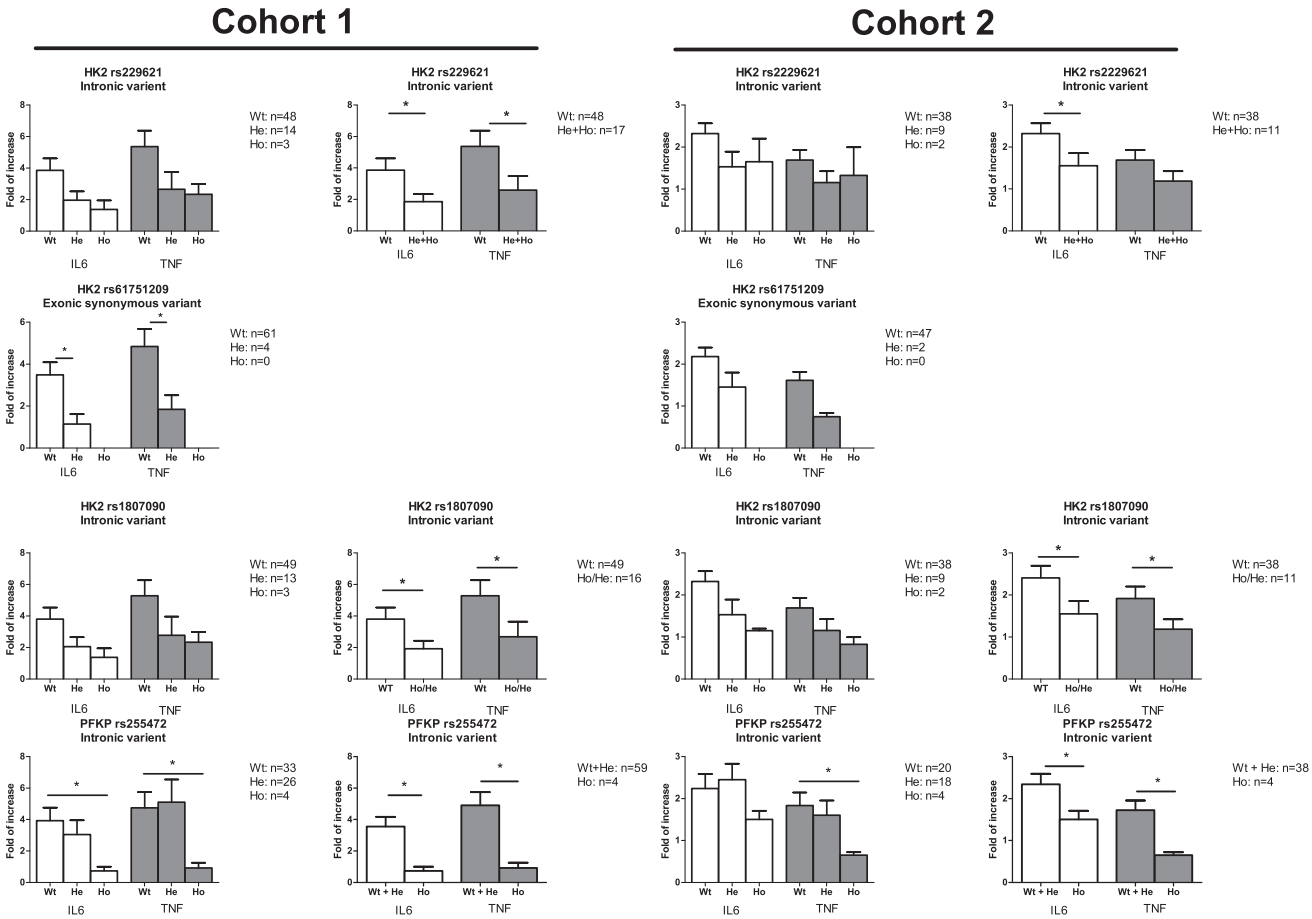

Figure 5. The Effect of SNPs in Glycolytic Genes on the Induction of Trained Immunity by BCG

Blood was drawn of healthy volunteers in 2011 (cohort 1) and 2015 (cohort 2) and SNPs were determined. Adherent monocytes were cultured in vitro as described in Figure 1A. Three SNPs in HK2 (rs2229621 and 1807090 in linkage disequilibrium, $R^2 = 0.936$) and one SNP in PFKP were found to affect the production of IL-6 and TNF-α in the supernatants upon LPS restimulation after BCG training in both cohorts (mean ± SEM). *$p < 0.05$, Wilcoxon signed-rank test.
See also Figure S5.

modulated the induction of trained immunity, and this effect was validated in the second cohort (Figure 5). Given the rate-limiting role of these enzymes for glycolysis, these findings support the essential role of glycolytic rate for the induction of trained immunity.

DISCUSSION

BCG-induced trained immunity results in an increased responsiveness of monocytes and macrophages, with effector functions such as cytokine production and reactive oxygen species release being increased upon secondary stimulation with non-related pathogens. Earlier studies have shown that trained immunity is caused by epigenetic rewiring at the chromatin level (Kleinnijenhuis et al., 2012). In this paper, we show that the change in inflammatory profile and the underlying epigenetic changes are dependent on changes in cellular metabolism, with an increase in glycolysis as central hallmark, but also with the upregulation of glutamine metabolism and oxidative phosphorylation. Furthermore, these metabolic changes were also epigenetically mediated, hence showing a complex interaction between immunometabolic pathways and epigenetic modifications.

The importance of cellular metabolism during immune cell activation has received a lot of attention in the last years. Already in the beginning of the past century, Otto Warburg showed that tumor cells displayed a higher rate of glycolysis and less oxidative phosphorylation compared to normal cells, a process called the Warburg effect (Warburg et al., 1927). More recently, a similar pattern has been described during activation of immune cells, such as for proinflammatory M(IFNγ) macrophages and activated lymphocytes (Pearce et al., 2013; Tan et al., 2015). Moreover, not only glucose metabolism but also other metabolic pathways play important roles in reprogramming and polarizing cells, with fatty acid oxidation and oxidative phosphorylation being essential for anti-inflammatory M(IL-4) macrophage polarization (Galván-Peña and O'Neill, 2014) and glutamine metabolism with succinate accumulation involved in IL-1β production (Tannahill et al., 2013). Recently, it was shown that the increase in glycolysis in LPS-activated bone-marrow-derived macrophages

(BMDMs) was also a result of altered activity of transcription factors, with a shift from Myc to HIF-1α-dependent transcriptional regulation (Liu et al., 2016).

In the present study, we demonstrate that cellular metabolism reprogramming is a central process involved in the induction of trained immunity by BCG vaccination as well. BCG is the most widely used vaccine worldwide, and many epidemiological studies have demonstrated its capacity to protect against non-mycobacterial infections as well (Aaby et al., 2011; Biering-Sørensen et al., 2012). We have recently shown that BCG is a potent inducer of trained immunity: understanding the pathways that contribute to this effect of BCG is, thus, crucial for understanding the induction of trained immunity in humans and, potentially, to design approaches for vaccination and immunotherapy in patients. Through a complementary approach combining in vitro experiments, BCG vaccination in mice, BCG proof-of-principle studies in humans, and genetic validation, we demonstrate a crucial role for the Akt/mTOR pathway inducing a high glycolytic rate for the induction of trained immunity. In addition, glutamine metabolism is also necessary for a full effective activation of trained immunity. In a model with β-glucan-induced trained immunity, a long-term increase in glycolysis (and pro-inflammatory phenotype) was also shown, which was also dependent on mTOR/HIF-1α pathway (Cheng et al., 2014). Interestingly, however, in β-glucan-induced trained immunity, a clear Warburg effect was seen, with a high glycolytic rate but decreased oxidative phosphorylation (Cheng et al., 2014). In contrast, BCG-induced trained immunity induced both glycolysis and an increase in oxygen consumption, arguing that different metabolic programs can be induced by various training stimuli. Nevertheless, when electron transport chain complex V was inhibited by oligomycin, no effect on cytokine production was observed, and when glucose metabolism was shifted from lactate production to the TCA cycle (by DCA), a decrease in induction of cytokine production was observed. This demonstrates that glycolytic rate and lactate production are more important for the induction of trained immunity than oxidative phosphorylation and that mitochondrial metabolism could be associated with carbon and not energy metabolism highlighted by the relevance of glutamine in trained immunity.

The effect of BCG on cellular metabolism has been little studied so far. In a BCG vaccination trial, PBMCs showed a decreased expression of glycolysis genes 2 days after vaccination, but they were upregulated at 7 and 14 days post-vaccination (Matsumiya et al., 2015). In our trial, we saw the upregulation of glycolysis genes and a trend for glutaminolysis genes up to 3 months after vaccination. However, this was performed in only 19 volunteers at one fixed time point after ex vivo stimulation. Given the strong variation in the human population, a larger trial with sequencing data (and, preferably, also genetic analysis) is strongly warranted. Furthermore, in infection models with *Mycobacterium tuberculosis* and *M. avium*, an overall shift of glucose metabolism from oxidative phosphorylation to fermentation (the Warburg effect) has been reported, and this was linked to pro-inflammatory cytokine production and bacterial survival (Appelberg et al., 2015; Gleeson et al., 2016; Shi et al., 2015). However, how long these shifts last and whether they are only an expression of the acute immune reaction to the mycobacteria are unknown.

One of the important conclusions of the present study is that these changes in cellular metabolism contribute to the long-term epigenetic reprogramming of trained monocytes. Previously, we have already shown how β-glucan-induced trained immunity results in metabolic changes (the Warburg effect), which is the result of epigenetic modulation, e.g., increased H3K4me3 and H3K27ac at promoter sites of essential glycolytic genes (Cheng et al., 2014). We have now confirmed that comparable epigenetic changes are induced in BCG-induced trained immunity. Interestingly, however, these epigenetic changes are, in turn, dependent on the induction of the metabolic pathways: if glycolysis or glutaminolysis is inhibited, changes in H3K4me3 and H3K9me3 at promoter sites of *IL6* and *TNFA* are reversed, showing a link between these two regulatory cellular processes. The relation between cellular metabolism and the epigenetic landscape of cells has recently received increased attention (Donohoe and Bultman, 2012; Hirschey et al., 2015; Kaelin and McKnight, 2013). Methylation of histone tails is regulated by lysine demethylases and histone methylstransferases, whose activity is influenced by cellular metabolites functioning as co-factors. For histone (and also DNA) methylation, S-adenosyl methionine (SAM), derived from methionine, serves as a methyl donor and co-factor (Kaelin and McKnight, 2013). More than 200 mammalian genes have been predicted to encode for SAM-dependent methyltransferases (Petrossian and Clarke, 2011). Unfortunately, the regulation of SAM in BCG-induced trained immunity is still unknown. Histone Lys demethylases (KDMs) of the JmjC and JmjD family need α-ketoglutarate as a co-factor for the demethylation process (Lu et al., 2012). Metabolites with a similar molecular structure—such as fumarate, succinate, or 2-hydroxyglutarate—can, in turn, serve as antagonizing factors (Lu et al., 2012; Xiao et al., 2012), thereby inhibiting the demethylation process. Moreover, these metabolites not only affect histone demethylases but also affect DNA demethylases (Xiao et al., 2012); therefore, this leaves DNA methylation and the effect of the changing metabolism on DNA methylation as an intriguing topic for future research. In this respect, it is important to point out that glutaminolysis, which can lead to succinate accumulation (Tannahill et al., 2013), when inhibited, abolished the upregulation of cytokine production by BCG. These data argue that the metabolic and epigenetic modifications are intertwined and that positive feedback loops are likely to strengthen the trained immunity phenotype. While we demonstrate here the impact of cellular metabolism on histone modifications at the level of immune gene promoters, epigenetic changes may be also induced in rate-limiting metabolic enzymes. Further study is needed to examine these possible effects.

In order to further demonstrate the importance of mTOR-dependent glycolysis for the induction of trained immunity, we show in a clinical trial that metformin (an mTOR inhibitor) administration can inhibit the induction of trained immunity. Finally, we demonstrate that genetic polymorphisms in genes encoding for the rate-limiting glycolysis enzymes HK2 and PFKP influence the induction of trained immunity in monocytes from two cohorts of healthy volunteers. Also, several SNPs in mTOR showed a tendency toward modulation of trained immunity, but their importance remains to be demonstrated in larger studies.

In conclusion, we show essential roles for glycolysis and glutamine metabolism for the induction of trained immunity in human monocytes by BCG. Induction of these pathways is regulated by epigenetic mechanisms at the level of chromatin organization. The next step should investigate the potential therapeutic role that the modulation of these pathways may have during vaccination.

EXPERIMENTAL PROCEDURES

Monocyte Isolation and Training Experiments

Buffy coats from healthy donors were obtained after written informed consent (Sanquin Blood Bank, Nijmegen, the Netherlands; and Hospital de Braga, Braga, Portugal). PBMC isolation was performed by dilution of blood in pyrogen-free PBS and differential density centrifugation over Ficoll-Paque density gradient media (GE Healthcare). Cells were washed twice in PBS and resuspended in RPMI culture medium (Invitrogen) supplemented with 50 μg/mL gentamicin, 2 mM glutamax (GIBCO), and 1 mM pyruvate (GIBCO). In some experiments, the glutamax was replaced with 2 mM or 1 mM L-glutamin (Sigma-Aldrich). Subsequently, monocyte isolation was performed by hyper-osmotic Percoll (Sigma) density gradient centrifugation. Afterward, cells were washed once with PBS. Monocytes were counted and adjusted to 1×10^6 cells per milliliter. A 100-μL volume was added to flat-bottomed 96-well plates (Corning), and cells were allowed to adhere for 1 hr at 37°C; subsequently, a washing step with 200 μL warm PBS was performed to yield maximal purity. Monocytes were incubated with culture medium only, as a negative control, or 5 μg/mL of BCG (SSI) for 24 hr (in 10% pooled human serum). Cells were washed once with 200 μL warm PBS and rested for 5 days in culture medium with 10% human pooled serum. Medium was changed once on day 3 of incubation. On day 6, cells were re-stimulated for 24 hr with 200 μL RPMI or 10 ng/mL *Escherichia coli* LPS (serotype 055:B5, Sigma-Aldrich), after which supernatants were collected and stored at −20°C. In some experiments, cells were pre-incubated (before BCG training) for 1 hr with 100 nM Wortmannin (Sigma), 10 nM rapamycin (Sigma), 50 μM BPTES (Sigma), 100 μM 6-aminonicotinamide (Sigma), 11 mM 2-deoxyglucose (Sigma), 0.3 mM metformin, 3 μM potassium dichloroacetate (DCA, Sigma), 1 mM AICAR (5-aminoimidazole-4-carboxamide-1-β-D-ribofuranoside, Brunschwig Chemie), 10 nM Torin 1 (R&D Systems), 1 μM oligomycin (Sigma).

Cytokine, Lactate, Glucose, and NAD^+ Measurements

Cytokine production was determined in supernatants using commercial ELISA kits for TNF-α (R&D Systems) and IL-6 (Sanquin), following the instructions of the manufacturer. Lactate, glucose, and NAD/NADH concentrations were measured using Fluorometric Quantification Assay Kits (Biovision).

Metabolite Measurements

10×10^6 monocytes were trained in 10-cm Petri dishes (Greiner) in 10-mL medium volumes. At day 6, cells were detached from the plate with Versene solution (Life Technologies) and counted. At least 1 million cells were lysed in 60 μL 0.5% Triton X-100 in PBS. Metabolite concentrations were determined by assay kits for fumarate, glutamate, malate, or acetyl-CoA (all Sigma), following the instructions of the manufacturer.

Western Blots

Monocytes were cultured as described earlier, and after 4 hr (Akt) or 6 days (mTOR), cells were lysed and stored at −80°C. Total protein amounts were determined by Pierce BCA Protein Assay Kit (Thermo Fisher Scientific), and equal amounts of proteins were loaded on precasted 4%–15% gels (Bio-Rad). The separated proteins were transferred to a nitrocellulose membrane (Bio-Rad), which was blocked in 5% BSA (Sigma). Incubation overnight at 4°C with rabbit polyclonal antibodies against phosphorylated (p-)Akt, p-mTOR, p-S6K, p-4EBP1 (Cell Signaling), and actin (Sigma) was used to determine the protein expression, which was visualized using a polyclonal secondary antibody (Dako) and SuperSignal West Femto Substrate (Thermo Fisher Scientific) or ECL (Bio-Rad).

mRNA Extraction and RT-PCR

Cells were cultured as described earlier. On day 6, mRNA was extracted by TRIzol (Life Technologies), according to the manufacturer's instructions, and cDNA was synthesized using iScript Reverse Transcriptase (Invitrogen). Relative expression was determined using the SYBR Green method (Invitrogen) on an Applied Biosciences StepOne PLUS qPCR machine, and the values are expressed as fold increases in mRNA levels, relative to those in non-trained cells, with HPRT as a housekeeping gene. Primers are listed in Table S1.

Chromatin Immunoprecipitation

10×10^6 monocytes were trained in 10-cm Petri dishes (Greiner) in 10-mL medium volumes. Cells were isolated and trained as described earlier. After resting for 5 days in culture medium, the cells were harvested and fixed in 1% methanol-free formaldehyde. Afterward, cells were sonicated, and immunoprecipitation was performed using antibodies against H3K4me3 and H3K9me3 (Diagenode). DNA was isolated with the MinElute PCR Purification Kit (QIAGEN) and was further processed for qPCR analysis using the SYBR Green method. Samples were analyzed by a comparative Ct method according to the manufacturer's instructions. The primers are listed in Table S1.

Assessment of Glycolysis and Oxygen Consumption by Seahorse Methodology

10×10^6 monocytes were trained in 10-cm Petri dishes (Greiner) in 10-mL medium volumes as described earlier and, after 6 days, were detached with Versene solution (ThermoFisher Scientific) from the culture plates. 100,000 cells in triplicate were plated to overnight-calibrated cartridges in assay medium (RPMI with 0.6 mM glutamine, [pH adjusted to 7.4]; for OCR, 5 mM glucose and 1 mM pyruvate were also added) and incubated for 1 hr in a non-CO_2-corrected incubator at 37°C. OCR and ECAR were analyzed using a Cell Mito Stress Kit (for OCR) or a glycolysis stress test (for ECAR) kit in an XFp Analyzer (Seahorse Bioscience), with final concentrations of 1 μM oligomycin, 1 μM FCCP, 0.5 μM rotenone/antimycin A, 10 mM glucose, and 50 mM 2-DG.

For Seahorse mouse ex vivo analyses, splenocytes were collected from either BCG-vaccinated or control mice and plated 4×10^5 cells per well in RPMI medium supplemented with 10% FBS. At 12 hr, cells were analyzed with a 96XFe analyzer to assess ECAR and OCR, as described earlier.

Animal Experiments

This article conforms to the relevant ethical guidelines for animal research. The research was approved by the Institutional Animal Care Committee of the Italian Ministry of Health (No. 220/2010-B), and the handling of mice was conducted in compliance with European Community Directive 86/609 and the American Association for Laboratory Animal Science's recommendations for the care and use of laboratory animals.

Briefly, C57BL/6 female mice were supplied as specific pathogen-free mice by Charles River Laboratories and were maintained in specific-pathogen-free conditions. Food and water were available ad libitum. 5 week-old mice were vaccinated, or not vaccinated, with a single dose of BCG (5×10^6 colony-forming units [CFU] in 200 μL PBS) injected intravenously (i.v.). Five mice were used for each experimental mouse group. Seven days after BCG vaccination, mice were sacrificed by cervical dislocation, in accordance with the ethics requirements, and spleens were aseptically collected. Single-cell suspensions were prepared in PBS by mechanic dissociation (gentleMACS dissociator) and applied to Falcon 2360 cell strainers (BD Discovery Labware) before being used in Seahorse experiments.

NMR and Amino Acid Experiments

Amino acids were quantified by high-performance liquid chromatography (HPLC) in a Gilson UV/VIS-155 detector (338 nm) after precolumn derivatization with ortho-phthalaldehyde (OPA, with methanol ≥ 99.9%, potassium borate [1 M, pH = 9.5], and 2-mercaptoethanol ≥ 99.0%) at a 1:5 ratio (Sigma-Aldrich). Culture supernatants were filtered by Acrodisc 13-mm syringe filters with a 0.2-μm Supor membrane (Pall Corporations). The inorganic mobile phase (pH = 7.8) was composed by a $Na_2HPO_4 \cdot 2H_2O_3$ (50 mM): propionic acid (250 mM) (1:1) mixture (Merck) with HPLC-grade acetonitrile in water (10:2:13). The organic mobile phase was composed by acetonitrile, methanol, and water (3:3:4) (HPLC grade, HiPerSolv Chromanorm, VWR

Chemicals). All mobile phases for elution were degasified for 30 min prior to analysis. Amino acids were quantified using the Gilson Uniprot software, version 5.11; and accordingly, standard solutions were prepared in MilliQ water (Millipore).

For NMR spectroscopy, methanol/water extracts and cell culture supernatants were analyzed. The aqueous and chloroform extracts were dried in a SpeedVac Plus system. The aqueous extract was suspended in 600 μL D_2O with 0.262 mM of TSP-d4 as chemical shift indicator and the organic extract in 600 μL CD_3Cl. To 550 μL cell culture media 50 μL D_2O was added, with a TSP-d4 final concentration of 0.262 mM.

The samples were analyzed at 25°C by ^1H NMR (nuclear magnetic resonance) and by 2D ^{13}C-^1H heteronuclear single-quantum coherence (HSQC) spectroscopy in an Ultrashield Plus 800 MHz spectrometer (Bruker) operating at 800.33 MHz, equipped with a TXI-Z H C/N/-D (5-mm) probe. The ^1H NMR pulse sequence used has a NOESY (nuclear Overhauser effect spectroscopy) presaturation (noesygppr1d) with irradiation at the water frequency (number of scans [ns] 124, time domain [TD] 64K, sweep width [SW] 20 ppm, relaxation delay [d1] 4 s, d8 0.01 s), while the ^{13}C-^1H HSQC used the hsqcetgpsisp2 pulse sequence (ns 16, TD1 512, TD2 2K, SW2 16 ppm, SW1 165 ppm, d1 1 s). The chemical shifts in the aqueous sample were referred to TSP (trimethylsilyl proprionate). Spectra were acquired and processed using TopSpin 3.2 software (Bruker); assignments were made by comparison with chemical shifts found in the literature for metabolic intermediates and Human Metabolome Database (http://www.hmdb.ca). The quantifications of the signals were performed by integration of the peaks in the 1H-NMR spectra and of the volumes in the ^{13}C-^1H-HSQC spectra, using the resonance due to the TSP as reference.

Ex Vivo Studies in Humans

In the BCG vaccination trial, 20 healthy volunteers were vaccinated with the BCG vaccine (SSI) after informed consent was obtained. Before vaccination and at 2 weeks post- and 3 months post-vaccination, blood was drawn and PBMCs were isolated and stimulated ex vivo with *M. tuberculosis*, *S. aureus*, or *C. albicans*. 24-hr supernatants were used to determine lactate production, and PBMCs were stored in TRIzol to determine gene expression. The study was approved by the Arnhem-Nijmegen Medical Ethical Committee (NL31936.091.10). Primary endpoints and detailed methods were published previously (Kleinnijenhuis et al., 2012).

In the metformin clinical trial, 12 healthy non-obese volunteers with good kidney function and devoid of metabolic disorders received increasing amounts of metformin for a total of 5 days (1,000 mg on day 1; 2,000 mg on day 6). Blood sampling was performed 1 day before the start of metformin (day 0), directly after metformin intake (day 6), on day 9, and on day 20 for ex vivo training of isolated monocytes. The study was approved by the Arnhem-Nijmegen Medical Ethical Committee (NL47793.091.14). Both studies were conducted in accordance with the Helsinki Declaration.

Genetic Analysis

For the genetic studies, we investigated genetic variation in two cohorts of healthy Dutch volunteers described previously (Li et al., 2016; Oosting et al., 2010, 2014): one cohort of 65 volunteers (cohort 1) collected in 2011, and a second cohort of 49 volunteers collected in 2015 (cohort 2). In both cohorts, we performed ex vivo trained immunity experiments. Volunteers were between 23 and 73 years old and consisted of 77% men and 23% women. Monocytes were cultured in vitro as described earlier. SNPs in the database for mTOR, HK2, PFKP, GLS, and GLUD1/2 were selected to analyze their effect on IL-6 and TNF-α production upon LPS restimulation after BCG training. SNP information was extracted from a genome-wide Illumina Infinium SNP array (Parkes et al., 2013). Linkage disequilibrium was calculated according to the methods of Machiela and Chanock (2015).

Statistics

Ex vivo and in vitro monocyte experiments were performed at least six times and analyzed using a Wilcoxon signed-rank test or one-way ANOVA, where applicable. A p value below 0.05 was considered statistically significant; $^*p < 0.05$, and $^{**}p < 0.01$. All data were analyzed using GraphPad prism 5.0. Data are shown as means ± SEM.

SUPPLEMENTAL INFORMATION

Supplemental Information includes five figures and one table and can be found with this article online at http://dx.doi.org/10.1016/j.celrep.2016.11.011.

AUTHOR CONTRIBUTIONS

Conceptualization: R.J.W.A., R.v.C., L.A.B.J., and M.G.N.; Methodology, R.J.W.A., E.L., J.K., M.O., C.P., C.L.R., A.C., F.R., R.S., L.G.G., A.B., C.C., R.v.C., and M.G.N.; Investigation, R.J.W.A., E.L., M.O., J.K., C.P., C.C., A.C., F.R., R.S., L.G.G., A.B., and C.L.R.; Writing – Original Draft, R.J.W.A.; Writing – Review & Editing, G.M., A.C., R.v.C., L.A.B.J., and M.G.N.; Supervision G.M., A.C., R.v.C., L.A.B.J., and M.G.N.

ACKNOWLEDGMENTS

M.G.N. was supported by an ERC consolidator grant (#310372) and a Spinoza prize of the Netherlands Organization for Scientific Research. A.C., F.R., and R.S. were supported by the Northern Portugal Regional Operational Programme (NORTE 2020), under the Portugal 2020 Partnership Agreement, through the European Regional Development Fund (FEDER) (NORTE-01-0145-FEDER-000013), and by the Fundação para a Ciência e Tecnologia (FCT) (IF/00735/2014 to A.C., IF/00021/2014 to R.S., and SFRH/BPD/96176/2013 to C.C.). L.G.G. was financially supported by Project LISBOA-01-0145-FEDER-007660 (Microbiologia Molecular, Estrutural e Celular), funded by FEDER funds through COMPETE2020 - Programa Operacional Competitividade e Internacionalização (POCI) and by national funds through the FCT (SFRH/BPD/111100/2015). The NMR spectrometers are part of the National NMR Facility supported by the FCT (RECI/BBB-BQB/0230/2012). G.M. was supported by an ERC starting grant (#310496).

Received: August 12, 2016
Revised: October 11, 2016
Accepted: October 31, 2016
Published December 6, 2016

REFERENCES

Aaby, P., Roth, A., Ravn, H., Napirna, B.M., Rodrigues, A., Lisse, I.M., Stensballe, L., Diness, B.R., Lausch, K.R., Lund, N., et al. (2011). Randomized trial of BCG vaccination at birth to low-birth-weight children: beneficial nonspecific effects in the neonatal period? J. Infect. Dis. *204*, 245–252.

Appelberg, R., Moreira, D., Barreira-Silva, P., Borges, M., Silva, L., Dinis-Oliveira, R.J., Resende, M., Correia-Neves, M., Jordan, M.B., Ferreira, N.C., et al. (2015). The Warburg effect in mycobacterial granulomas is dependent on the recruitment and activation of macrophages by interferon-γ. Immunology *145*, 498–507.

Arts, R.J., Blok, B.A., Aaby, P., Joosten, L.A., de Jong, D., van der Meer, J.W., Benn, C.S., van Crevel, R., and Netea, M.G. (2015a). Long-term in vitro and in vivo effects of γ-irradiated BCG on innate and adaptive immunity. J. Leukoc. Biol. *98*, 995–1001.

Arts, R.J., Blok, B.A., van Crevel, R., Joosten, L.A., Aaby, P., Benn, C.S., and Netea, M.G. (2015b). Vitamin A induces inhibitory histone methylation modifications and down-regulates trained immunity in human monocytes. J. Leukoc. Biol. *98*, 129–136.

Biering-Sørensen, S., Aaby, P., Napirna, B.M., Roth, A., Ravn, H., Rodrigues, A., Whittle, H., and Benn, C.S. (2012). Small randomized trial among low-birth-weight children receiving bacillus Calmette-Guérin vaccination at first health center contact. Pediatr. Infect. Dis. J. *31*, 306–308.

Cairns, R.A., Papandreou, I., Sutphin, P.D., and Denko, N.C. (2007). Metabolic targeting of hypoxia and HIF1 in solid tumors can enhance cytotoxic chemotherapy. Proc. Natl. Acad. Sci. USA *104*, 9445–9450.

Cheng, S.C., Quintin, J., Cramer, R.A., Shepardson, K.M., Saeed, S., Kumar, V., Giamarellos-Bourboulis, E.J., Martens, J.H., Rao, N.A., Aghajanirefah, A.,

et al. (2014). mTOR- and HIF-1α-mediated aerobic glycolysis as metabolic basis for trained immunity. Science *345*, 1250684.

Cheng, S.C., Scicluna, B.P., Arts, R.J., Gresnigt, M.S., Lachmandas, E., Giamarellos-Bourboulis, E.J., Kox, M., Manjeri, G.R., Wagenaars, J.A., Cremer, O.L., et al. (2016). Broad defects in the energy metabolism of leukocytes underlie immunoparalysis in sepsis. Nat. Immunol. *17*, 406–413.

Colditz, G.A., Brewer, T.F., Berkey, C.S., Wilson, M.E., Burdick, E., Fineberg, H.V., and Mosteller, F. (1994). Efficacy of BCG vaccine in the prevention of tuberculosis. Meta-analysis of the published literature. JAMA *271*, 698–702.

Donohoe, D.R., and Bultman, S.J. (2012). Metaboloepigenetics: interrelationships between energy metabolism and epigenetic control of gene expression. J. Cell. Physiol. *227*, 3169–3177.

Galván-Peña, S., and O'Neill, L.A. (2014). Metabolic reprograming in macrophage polarization. Front. Immunol. *5*, 420.

Garly, M.L., Martins, C.L., Balé, C., Baldé, M.A., Hedegaard, K.L., Gustafson, P., Lisse, I.M., Whittle, H.C., and Aaby, P. (2003). BCG scar and positive tuberculin reaction associated with reduced child mortality in West Africa. A non-specific beneficial effect of BCG? Vaccine *21*, 2782–2790.

Gleeson, L.E., Sheedy, F.J., Palsson-McDermott, E.M., Triglia, D., O'Leary, S.M., O'Sullivan, M.P., O'Neill, L.A., and Keane, J. (2016). Cutting edge: Mycobacterium tuberculosis induces aerobic glycolysis in human alveolar macrophages that is required for control of intracellular bacillary replication. J. Immunol. *196*, 2444–2449.

Hirschey, M.D., DeBerardinis, R.J., Diehl, A.M., Drew, J.E., Frezza, C., Green, M.F., Jones, L.W., Ko, Y.H., Le, A., Lea, M.A., et al.; Target Validation Team (2015). Dysregulated metabolism contributes to oncogenesis. Semin. Cancer Biol. *35* (*Suppl*), S129–S150.

Kaelin, W.G., Jr., and McKnight, S.L. (2013). Influence of metabolism on epigenetics and disease. Cell *153*, 56–69.

Kleinnijenhuis, J., Quintin, J., Preijers, F., Joosten, L.A., Ifrim, D.C., Saeed, S., Jacobs, C., van Loenhout, J., de Jong, D., Stunnenberg, H.G., et al. (2012). Bacille Calmette-Guerin induces NOD2-dependent nonspecific protection from reinfection via epigenetic reprogramming of monocytes. Proc. Natl. Acad. Sci. USA *109*, 17537–17542.

Kristensen, I., Aaby, P., and Jensen, H. (2000). Routine vaccinations and child survival: follow up study in Guinea-Bissau, West Africa. BMJ *321*, 1435–1438.

Li, Y., Oosting, M., Deelen, P., Ricano-Ponce, I., Smeekens, S., Jaeger, M., Matzaraki, V., Swertz, M.A., Xavier, R.J., Franke, L., et al. (2016). Inter-individual variability and genetic influences on cytokine responses to bacteria and fungi. Nat. Med.

Liu, L., Lu, Y., Martinez, J., Bi, Y., Lian, G., Wang, T., Milasta, S., Wang, J., Yang, M., Liu, G., et al. (2016). Proinflammatory signal suppresses proliferation and shifts macrophage metabolism from Myc-dependent to HIF1α-dependent. Proc. Natl. Acad. Sci. USA *113*, 1564–1569.

Lu, C., Ward, P.S., Kapoor, G.S., Rohle, D., Turcan, S., Abdel-Wahab, O., Edwards, C.R., Khanin, R., Figueroa, M.E., Melnick, A., et al. (2012). IDH mutation impairs histone demethylation and results in a block to cell differentiation. Nature *483*, 474–478.

Machiela, M.J., and Chanock, S.J. (2015). LDlink: a web-based application for exploring population-specific haplotype structure and linking correlated alleles of possible functional variants. Bioinformatics *31*, 3555–3557.

Matsumiya, M., Satti, I., Chomka, A., Harris, S.A., Stockdale, L., Meyer, J., Fletcher, H.A., and McShane, H. (2015). Gene expression and cytokine profile correlate with mycobacterial growth in a human BCG challenge model. J. Infect. Dis. *211*, 1499–1509.

Netea, M.G., Quintin, J., and van der Meer, J.W. (2011). Trained immunity: a memory for innate host defense. Cell Host Microbe *9*, 355–361.

Netea, M.G., Joosten, L.A., Latz, E., Mills, K.H., Natoli, G., Stunnenberg, H.G., O'Neill, L.A., and Xavier, R.J. (2016). Trained immunity: A program of innate immune memory in health and disease. Science *352*, aaf1098.

Odegaard, J.I., and Chawla, A. (2011). Alternative macrophage activation and metabolism. Annu. Rev. Pathol. *6*, 275–297.

Oosting, M., Berende, A., Sturm, P., Ter Hofstede, H.J., de Jong, D.J., Kanneganti, T.D., van der Meer, J.W., Kullberg, B.J., Netea, M.G., and Joosten, L.A. (2010). Recognition of Borrelia burgdorferi by NOD2 is central for the induction of an inflammatory reaction. J. Infect. Dis. *201*, 1849–1858.

Oosting, M., Cheng, S.C., Bolscher, J.M., Vestering-Stenger, R., Plantinga, T.S., Verschueren, I.C., Arts, P., Garritsen, A., van Eenennaam, H., Sturm, P., et al. (2014). Human TLR10 is an anti-inflammatory pattern-recognition receptor. Proc. Natl. Acad. Sci. USA *111*, E4478–E4484.

Parkes, M., Cortes, A., van Heel, D.A., and Brown, M.A. (2013). Genetic insights into common pathways and complex relationships among immune-mediated diseases. Nat. Rev. Genet. *14*, 661–673.

Pearce, E.L., Poffenberger, M.C., Chang, C.H., and Jones, R.G. (2013). Fueling immunity: insights into metabolism and lymphocyte function. Science *342*, 1242454.

Pereira, L.I., Dorta, M.L., Pereira, A.J., Bastos, R.P., Oliveira, M.A., Pinto, S.A., Galdino, H., Jr., Mayrink, W., Barcelos, W., Toledo, V.P., et al. (2009). Increase of NK cells and proinflammatory monocytes are associated with the clinical improvement of diffuse cutaneous leishmaniasis after immunochemotherapy with BCG/Leishmania antigens. Am. J. Trop. Med. Hyg. *81*, 378–383.

Petrossian, T.C., and Clarke, S.G. (2011). Uncovering the human methyltransferasome. Mol. Cell Proteomics *10*, M110.000976.

Quintin, J., Saeed, S., Martens, J.H., Giamarellos-Bourboulis, E.J., Ifrim, D.C., Logie, C., Jacobs, L., Jansen, T., Kullberg, B.J., Wijmenga, C., et al. (2012). Candida albicans infection affords protection against reinfection via functional reprogramming of monocytes. Cell Host Microbe *12*, 223–232.

Roth, A., Gustafson, P., Nhaga, A., Djana, Q., Poulsen, A., Garly, M.L., Jensen, H., Sodemann, M., Rodriques, A., and Aaby, P. (2005). BCG vaccination scar associated with better childhood survival in Guinea-Bissau. Int. J. Epidemiol. *34*, 540–547.

Rousseau, M.C., Parent, M.E., and St-Pierre, Y. (2008). Potential health effects from non-specific stimulation of the immune function in early age: the example of BCG vaccination. Pediatr. Allergy Immunol. *19*, 438–448.

Saeed, S., Quintin, J., Kerstens, H.H., Rao, N.A., Aghajanirefah, A., Matarese, F., Cheng, S.C., Ratter, J., Berentsen, K., van der Ent, M.A., et al. (2014). Epigenetic programming of monocyte-to-macrophage differentiation and trained innate immunity. Science *345*, 1251086.

Salem, A., Nofal, A., and Hosny, D. (2013). Treatment of common and plane warts in children with topical viable Bacillus Calmette-Guerin. Pediatr. Dermatol. *30*, 60–63.

Shi, L., Salamon, H., Eugenin, E.A., Pine, R., Cooper, A., and Gennaro, M.L. (2015). Infection with Mycobacterium tuberculosis induces the Warburg effect in mouse lungs. Sci. Rep. *5*, 18176.

Tan, Z., Xie, N., Cui, H., Moellering, D.R., Abraham, E., Thannickal, V.J., and Liu, G. (2015). Pyruvate dehydrogenase kinase 1 participates in macrophage polarization via regulating glucose metabolism. J. Immunol. *194*, 6082–6089.

Tannahill, G.M., Curtis, A.M., Adamik, J., Palsson-McDermott, E.M., McGettrick, A.F., Goel, G., Frezza, C., Bernard, N.J., Kelly, B., Foley, N.H., et al. (2013). Succinate is an inflammatory signal that induces IL-1β through HIF-1α. Nature *496*, 238–242.

van 't Wout, J.W., Poell, R., and van Furth, R. (1992). The role of BCG/PPD-activated macrophages in resistance against systemic candidiasis in mice. Scand. J. Immunol. *36*, 713–719.

Warburg, O., Wind, F., and Negelein, E. (1927). The metabolism of tumors in the body. J. Gen. Physiol. *8*, 519–530.

Xiao, M., Yang, H., Xu, W., Ma, S., Lin, H., Zhu, H., Liu, L., Liu, Y., Yang, C., Xu, Y., et al. (2012). Inhibition of α-KG-dependent histone and DNA demethylases by fumarate and succinate that are accumulated in mutations of FH and SDH tumor suppressors. Genes Dev. *26*, 1326–1338.

Zumla, A., Raviglione, M., Hafner, R., and von Reyn, C.F. (2013). Tuberculosis. N. Engl. J. Med. *368*, 745–755.

Cell Reports, Volume *17*

Supplemental Information

Immunometabolic Pathways in BCG-Induced Trained Immunity

Rob J.W. Arts, Agostinho Carvalho, Claudia La Rocca, Carla Palma, Fernando Rodrigues, Ricardo Silvestre, Johanneke Kleinnijenhuis, Ekta Lachmandas, Luís G. Gonçalves, Ana Belinha, Cristina Cunha, Marije Oosting, Leo A.B. Joosten, Giuseppe Matarese, Reinout van Crevel, and Mihai G. Netea

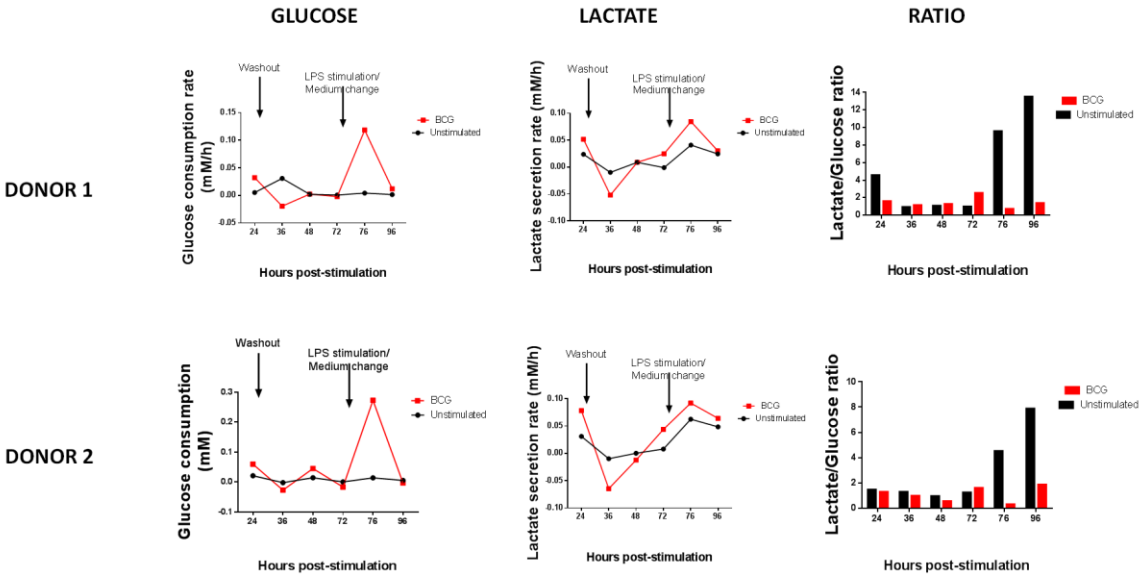

Figure S1. Glucose metabolism, Related to Figure 1. Human monocytes were trained for 24h with BCG or left in medium as control. After 2 subsequent days rest, cells were restimulated with LPS. Glucose consumption and lactate production in the medium were assessed at different time points for 2 donors and lactate:glucose ratios were calculated.

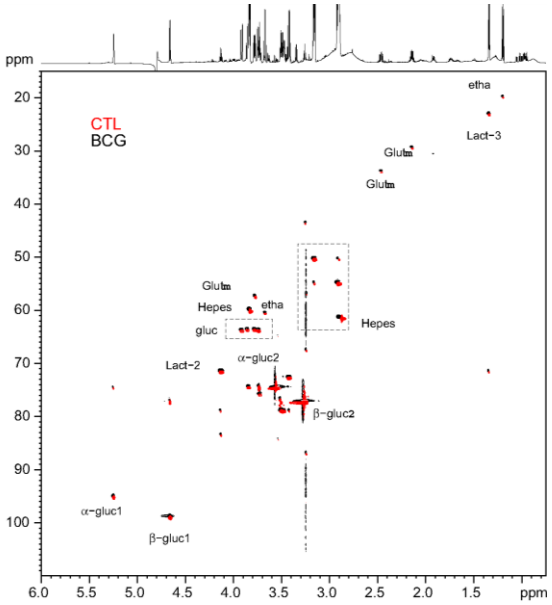

Figure S2. Related to Figure 1 and S3. (A) Spectrum of culture media. Representative ^{13}C-^{1}H-HSQC spectrum of the culture media of human monocytes trained for 24h with BCG (BCG; red) or left in medium as control (CTL; black) following a subsequent 24h incubation with LPS in the presence of 2-^{13}C-labeled glucose. The 2D-spectrum shows the proton resonances (X-axis) directly linked to ^{13}C (Y-axis), with the resonances of 2-^{13}C-glucose (Gluc-2) and 2-^{13}C-lactate (Lact-2) being the more intense (see Figure S3). The chemical shift is expressed in parts per million (ppm). The spectrum displays other peaks corresponding to other compounds that are not resulting from the metabolism of 2-^{13}C-labeled glucose. Gluc- glucose; Glutm- glutamine; Lact- lactate; etha- ethanol.

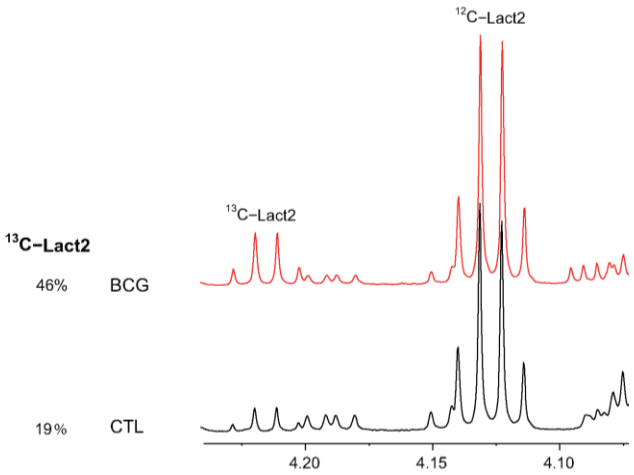

(B) Spectrum of cell extracts. Highlight of a representative 2-lactate ^{1}H-NMR spectrum of cell extracts from human monocytes trained for 24h with BCG (BCG; red) or left in medium as control (CTL; black) following a subsequent 24h incubation with LPS in the presence of 2-^{13}C-labeled glucose. The presence of a ^{13}C splits the resonances of the protons directly linked in two by a *J*-coupling constant, allowing the calculation of the ^{13}C incorporated in each position in comparison with ^{12}C-lactate abundance (≈ 4.15-4.10 ppm). In the case of the position 2 of lactate, the total incorporation of ^{13}C from the 2-^{13}C-glucose is 19 % in the control macrophages and 46% in the BCG-trained macrophages.

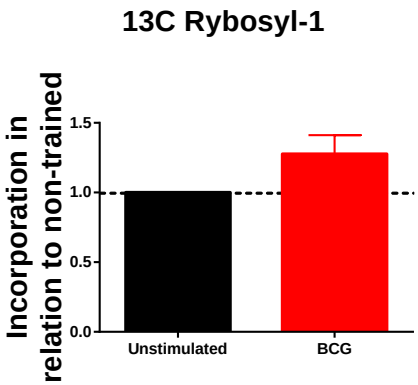

(C) ^{13}C-labeled glucose incorportation in Rybosyl. Human monocytes were trained for 24h with BCG or left in medium as control. After 2 subsequent days rest, cells were restimulated with LPS in medium with ^{13}C-labeled glucose. After 24h incorportation in intracellular metabolites was assessed. (Mean ± SD, n=3).

A.

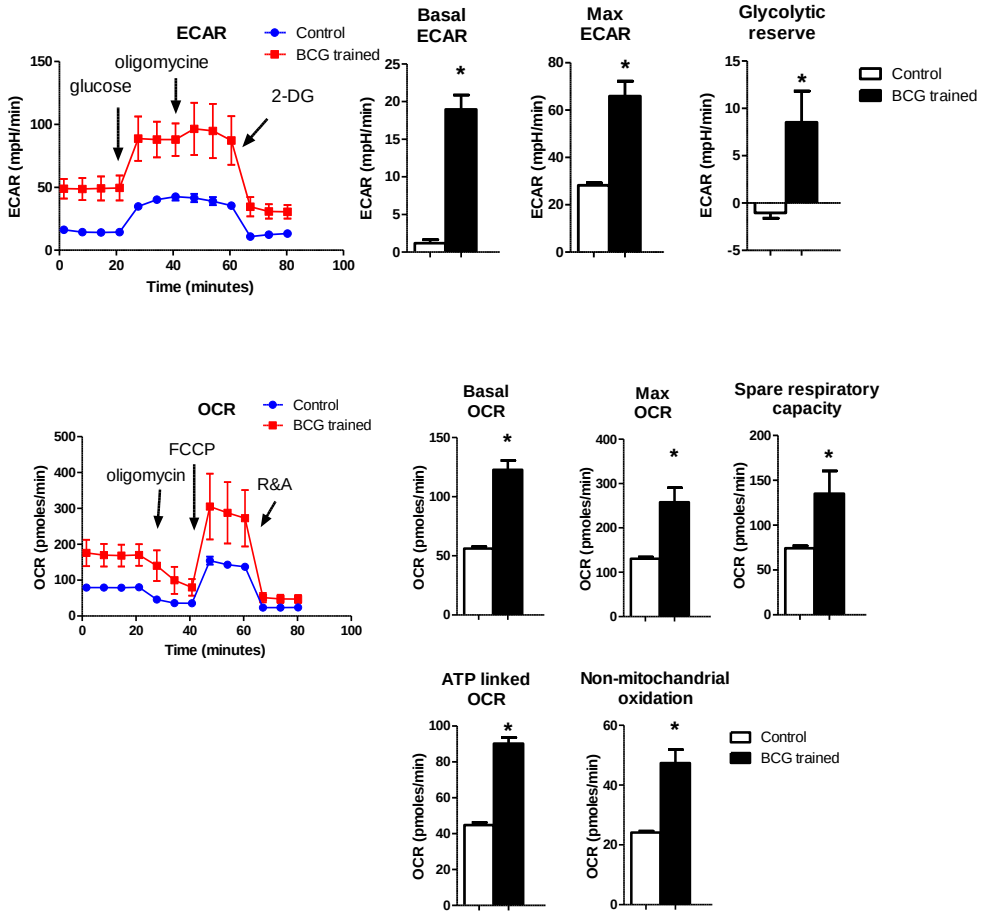

B.

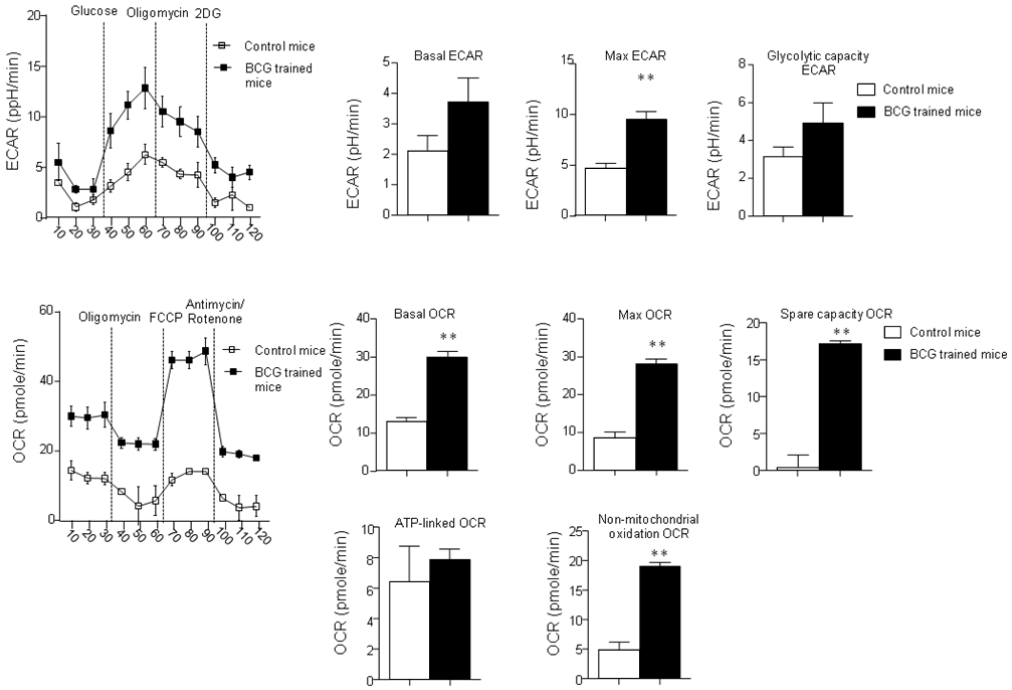

Figure S3. Related to Figure 1C,D. (A) Complete human Seahorse data. Monocytes were incubated for 24h with culture medium or BCG. At day 6 (prior to restimulation) extracellular acidification rate (ECAR) and oxygen consumption rate (OCR) were determined by Seahorse. (Mean ± SEM, n=6, * P < 0.05, Wilcoxon signed-rank test). (B) Complete mice Seahorse data. Mice were vaccinated with BCG. After 7 days splenocytes were isolated and ECAR and OCR were determined by Seahorse. (Mean ± SEM, n=6, * P < 0.05, ** P < 0.01, Mann-Whitney test).

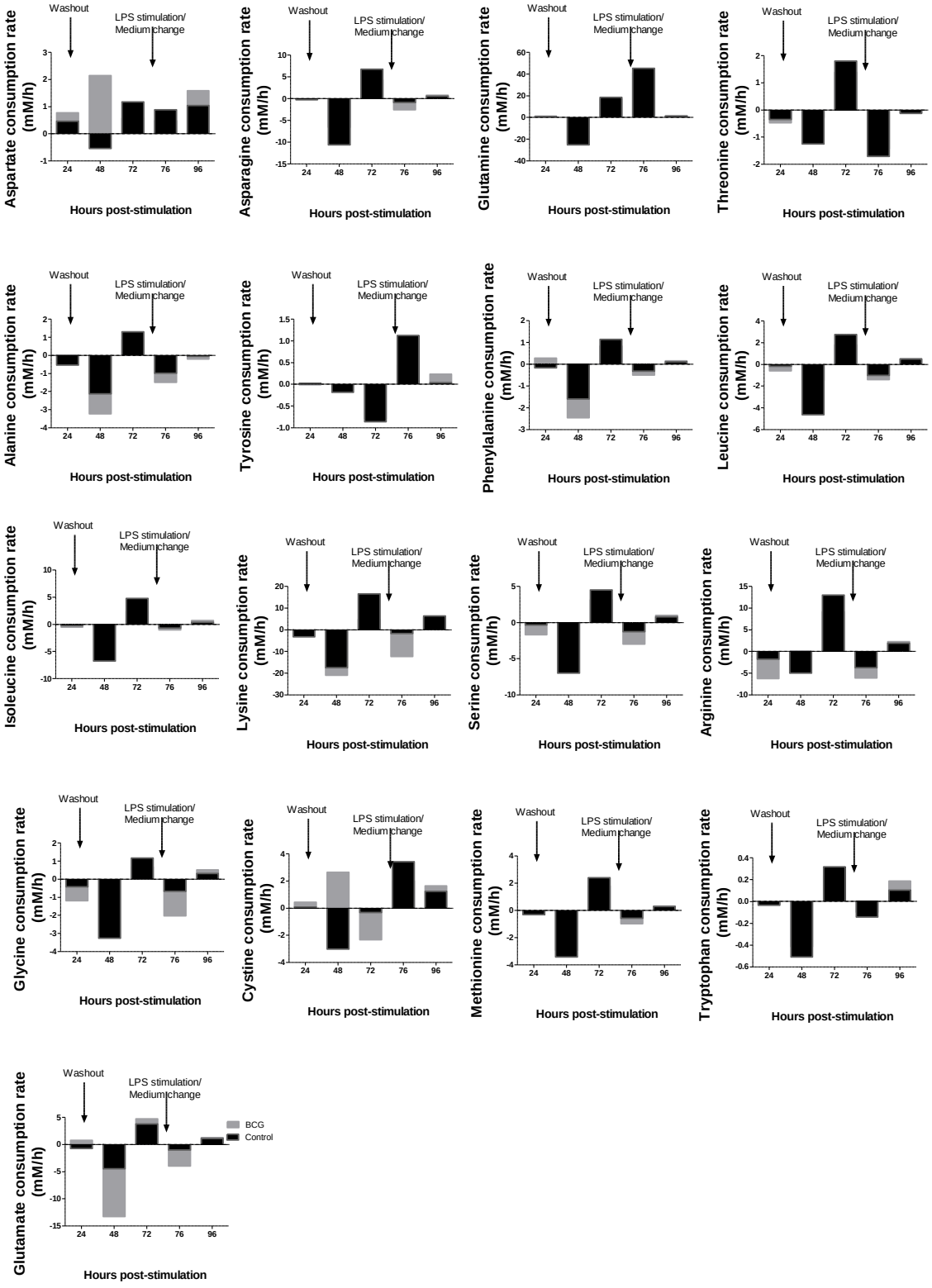

Figure S4. Related to Figure 1. Amino acid consumption from medium. Human monocytes were trained for 24h with BCG or left in medium as control. After 2 subsequent days rest, cells were restimulated with LPS. Amino acid consumption from the medium was assessed at the indicated time points.

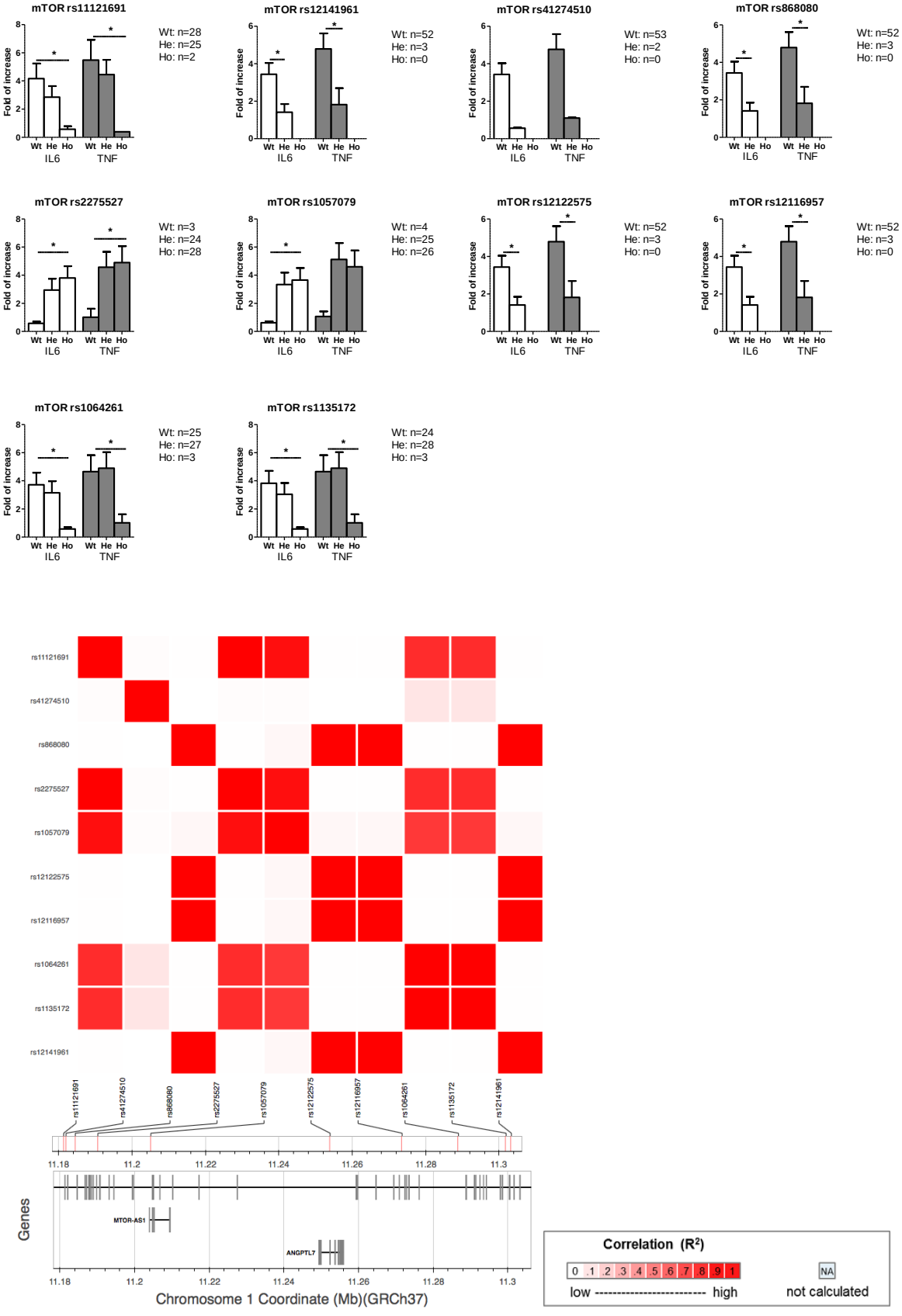

Figure S5. Related to Figure 5. Effect of mTOR SNPs on induction of trained immunity. Blood was drawn of healthy volunteers in 2011 (cohort 1) and SNPs were determined. Adherent monocytes were cultured in vitro as described in figure 1A. The indicated SNPs in mTOR were found to affect the production of IL-6 and TNF upon LPS restimulation after BCG training. (Mean ± SEM, * $P < 0.05$, Wilcoxon signed-rank test). Linkage disequilibria of the displayed mTOR SNPs. Calculated according to the methods of Machiela and Chanock. (Machiela and Chanock, 2015)

Epigenetic promoter primers		
Gene	Forward (5'-->3')	Reverse (5'-->3')
Myoglobulin	AGCATGGTGCCACTGTGCT	GGCTTAATCTCTGCCTCATGAT
H2B	TGTACTTGGTGACGGCCTTA	CATTACAACAAGCGCTCGAC
GAPDH	CCCCGGTTTCTATAAATTGAGC	AAGAAGATGCGGCTGACTGT
ZNF UTR	AAGCACTTTGACAACCGTGA	GGAGGAATTTTGTGGAGCAA
TNF	GTGCTTGTTCCTCAGCCTCT	ATCACTCCAAAGTGCAGCAG
IL6	AGGGAGAGCCAGAACACAGA	GAGTTTCCTCTGACTCCATCG
mTOR	ATAAAGAGCGCTAGCCCGAA	GACCCCTCCCGGTGTAATTC
HK2	GAGCTCAATTCTGTGTGGAGT	ACTTCTTGAGAACTATGTACCCTT
PFKP	CGAAGGCGATGGGGTGAC	CATCGCTTCGCCACCTTTC
GLS	CCAGAGCCCCTAGTACCCAA	TTGGCGATTAGGGCAGTCAA
GLUD	GAAGTCCGTCCTCCCCGTTA	TTTTAAGCCGCAGCTTCCTG
qPCR primers		
Gene	Forward (5'-->3')	Reverse (5'-->3')
HPRT	CCTGGCGTCGTGATTAGTGAT	AGACGTTCAGTCCTGTCCATAA
mTOR	TCCGAGAGATGAGTCAAGAGG	CACCTTCCACTCCTATGAGGC
HK2	TTGACCAGGAGATTGACATGGG	CAACCGCATCAGGACCTCA
PFKP	ATTGCGGTTTTCGATGCCAC	GCCACAACTGTAGGGTCGT
GLS	AGGGTCTGTTACCTAGCTT	ACGTTCGCAATCCTGTAGA
GLUD	TCGTGGAGGACAAGTTGGT	TTGCAGGGCTTGATGATCC

Table S1. Related to Figure 3. Used primers.

Supplementary references

Machiela, M.J., and Chanock, S.J. (2015). LDlink: a web-based application for exploring population-specific haplotype structure and linking correlated alleles of possible functional variants. Bioinformatics *31*, 3555-3557.